IEEE Access
Multidisciplinary | Rapid Review | Open Access Journal

Received July 21, 2021, accepted August 8, 2021, date of publication August 16, 2021, date of current version September 1, 2021.

Digital Object Identifier 10.1109/ACCESS.2021.3105382

An Improved Forest Fire Monitoring Algorithm With Three-Dimensional Otsu

ZHAO DENG AND GUI ZHANG
School of Forestry, Central South University of Forestry and Technology, Changsha 410004, China
Corresponding author: Gui Zhang (2430896569@qq.com)

This work was supported in part by the Science and Technology Innovation Platform and Talent Plan Project of Hunan Province under Grant 2017TP1022, and in part by the Emergency Management Science and Technology Project of Hunan Province under Grant 2020YJ007.

ABSTRACT Forest fires can destroy millions of acres of land at shockingly fast speeds. The forest fire points identification algorithm is the most critical step in the forest fire monitoring process. Most traditional forest fire monitoring methods use fixed thresholds, ignoring background pixels, and have low recognition rates, which could lead to many problems, such as false reporting and low recognition rate. This paper proposes and tests an adaptive forest fire points identification algorithm using Himawari-8 data. By calculating the three-dimensional histogram of brightness temperature, an adaptive threshold that can automatically identify potential forest fire points is obtained. Based on this three-dimensional Otsu method, the contextual test algorithm has also been adopted to specify forest fire points. The experimental results show that the omission rate of the improved algorithm is about 10% lower than that of the previous algorithm in small-scale fire incidents. The improved algorithm can quickly and effectively extract fire point information, and it is also sensitive to small and low-temperature fires, which provides an efficient means for monitoring fire disasters.

INDEX TERMS Himawari-8 geostationary satellite, forest fires monitoring, 3D Otsu algorithm, adaptive dynamic threshold, image segmentation, brightness temperature.

I. INTRODUCTION

Protecting and developing forest resources are the signs of human needs and the progress of social civilization [1]. Among the factors that harm forests, fire is the most serious one. Forest fire is a natural disaster that is sudden, destructive, difficult to control, and can cause huge losses to humans and ecosystems [2]. Because remote sensing satellites have the advantages of low cost, wide coverage area, and strong real-time performance, they have been the most effective tool for detecting forest fires in the past forty years [3], [4]. Due to the limitation of time intervals of passing territory of polar-orbiting satellites [5], the geostationary satellites with high temporal resolution which can uninterruptedly monitor forest fire occurrences are of importance. The last ten years, researchers have been using Fires Low Earth Orbiting (LEO) and geostationary satellite data to monitor fires [6], [7]. Due to the advantages of being real-time and having a fixed detection location, the geostationary satellite (Himawari-8) can continuously obtain fire sites in the monitoring of forest fires. This information is of great significance for detecting fires, fighting forest fires, and reducing the negative impact of disasters [8]. Therefore, this paper proposes a new type of forest fire monitoring algorithm with higher accuracy based on Himawari-8, an advanced geostationary satellite in Asia.

The forest fire points identification algorithm is the most critical step in the forest fire monitoring process. According to the current domestic and foreign research, the forest fire points identification algorithms based on polar orbit satellite data are mainly applied in five methods: the spectral method, the multi-temporal detection method, the fuel mask method, the threshold method and the contextual method [9], [10]. The original spectral method has many limitations because it is based on the following assumptions: (1) the fire pixel and the background pixel are uniform temperature fields. (2) the atmospheric influence is ignored. (3) the pixel is unsaturated in both channels used to identify fire (3.75μm and 10.8μm). Although Pan *et al.* [11] took into account the influence of the atmosphere and the reflection of the sun on the smaller surface in the daytime image, and improved the spectral method that is more in line with the reality, the method still cannot produce corresponding effects in the complex actual environment. Filizzola *et al.* [12] proposed a robust satellite technology for fire detection, RST-FIRES. The algorithm

The associate editor coordinating the review of this manuscript and approving it for publication was John Xun Yang.

uses multi-temporal data in the same area to monitor the fire in real time. When a pixel is ''abnormal'', this method will recognize it as a fire point pixel. The disadvantage of this method is that it is very susceptible to cloud influence. The fuel mask method refers to the normalized difference vegetation index (NDVI) to reflect the vegetation coverage rate on the ground, and identify whether there is enough combustible materials in the pixel according to the preset threshold. Jie *et al.* [13] improved the original fuel mask method and constructed a fire spot recognition algorithm based on brightness temperature, vegetation index and AOD. In these five methods, the threshold method proposed by Flannigan and Vonder [14] and the contextual method by Flasse *et al.* [15] are the most widely used. The absolute threshold method is to identify forest fire points by setting a fixed threshold. The fixed threshold is used to distinguish the brightness temperature of fire and non-fire points, but this method would be affected by environmental differences in different areas and cause inaccurate recognition results [16]. Considering that the fire point information and the neighboring area information would bring a low false alarm rate, Giglio *et al.* [3] put forward a method that the contextual fire point detection algorithm that applied to MODIS data. Nonetheless, this algorithm still uses a fixed potential threshold to identify potential fire points, which will greatly affect the results of forest fire points monitoring. Moreover, in practice, different areas and different environmental conditions will lead to different threshold values for potential fire points [17], [18]. Owing to the above shortcomings, Du tried to calculate the gradient line in the TIR data to find a flexible threshold value [19]. At the same time, Giglio also set a dynamic threshold by scanning the average value of each MODIS data sample [4]. However, these fire point monitoring methods based on a single type of value are not sufficiently adaptable to different areas, and a more flexible threshold calculation method is required.

Using image segmentation to automatically find potential thresholds can make up for the shortcomings of existing contextual forest fire monitoring algorithms. The Otsu method is used to segment the background and the target in the image. It uses the between-class variance as a basis, and selects the gray value that maximizes the between-class variance as the best threshold to extract the target from the background [20]. When this method has been applied to forest fires monitoring, it is possible to extract the fire point from the background more accurately because the greater the difference between the fire point and the background characteristic value, the greater the variance between clusters. When the variance between clusters reaches a certain value, the two have good distinguishability, and we can get better results [21]. However, one of the major limitations of this method is that the threshold segmentation method based on the one-dimensional image only reflects the gray level information of a single pixel of the image, and fail to consider the neighborhood information between other pixels such as space [22]. To overcome this issue, Zhang *et al.* [23] applied the Otsu method to high-voltage electric fires, and took into account the value of the pixel and the relationship between the pixels in its field, extending the one-dimensional histogram to the two-dimensional histogram. Although the two-dimensional histogram oblique division method improves the area division, but under the influence of high-intensity noise, there are more misclassifications, resulting in poor segmentation results. On this basis, this paper takes the median gray level information as a third feature and integrates it into the existing two-dimensional histogram to construct a 3D gray histogram to calculate the forest fire point threshold of the pixel.

This paper uses image segmentation technology — three-dimensional Otsu method — to automatically select the threshold of potential fire pixels, and then uses the potential dynamic threshold to identify potential fire pixels, which is more adaptive and optimizes the existing contextual fire detection algorithm. This algorithm solves the problem of wrong forest fire points detection caused by the fixed threshold, which is not suitable for certain areas. It is also more accurate and sensitive to the identification of fire points. The main modules of the proposed method are constructed around an analysis of Himawari-8 data. At the same time, the design can also be applied to other similar sensors to take full advantage of the data and reduce false alarm to a minimum.

The paper includes five sections. The second section briefly introduces the area and data used in current study. The third section describes in detail the improved contextual forest fire point detection algorithm proposed in this paper. The fourth section tests and discusses the algorithm, and combines accuracy rate and missed detection rate to evaluate the algorithm comprehensively. Finally, the conclusion is placed in section 5.

II. STUDY AREA AND DATA SOURCES

A. STUDY AREA

The study was carried out in Yunnan province in China, which is bounded by latitude (N) 21°08′32″—29°15′08″ and longitude (E) 97°31′39″—106°11′47″. It belongs to low-latitude and high-altitude regions with diverse climate types. Regional climate differences and vertical variations are obvious. The annual temperature difference is small, but the daily temperature difference is large. There are dry and wet seasons, and the average annual rainfall is about 1100mm, in spite of the uneven space distribution. Spring and winter are the fire-prone seasons in most parts of Yunnan Province. In addition, Yunnan pine trees, one of the main tree species in the whole province, are easily flammable, which also increase the probability of forest fires.

B. DATA

Himawari-8 satellite carries the world's advanced AHI (Advanced Himawari Imager) imager. The temporal resolution of the entire observation is 10 min once, and that of Japan and specific target areas can reach 2.5 min. It includes

FIGURE 1. Yunnan province study.

16 channels (Table 1), ranging from visible light to infrared light. There are three visible light channels (channel 1, 2, 3), and the highest spatial resolution is 500m. There are 13 near-infrared and infrared channels, which can provide accurate meteorological and ground observation information [24]. As Himawari-8 satellite can accurately locate fire spots within 1 pixel, it would meet the requirements in actual fire monitoring.

The theoretical basis of satellite remote sensing fire spot identification is the relationship between temperature and radiation wavelength. Wien's displacement law defines it as the relationship between the blackbody radiation wavelength λ_m and the blackbody temperature T, defined as

$$T\lambda_m = B \tag{1}$$

B is the Wien displacement constant and the value is $2.897 \times 10^{-3}\mu$m·K. When a fire occurs, the temperature of the black body gradually increases, and the wavelength of the electromagnetic wave radiated by the black body becomes shorter. Since the mid-infrared is more sensitive to the high temperature response than the thermal infrared, the peak wavelength will move to the short-wave direction with the increase of temperature. Therefore, when a fire occurs, the brightness temperature of the channel near 4 μm increases rapidly, while the response of the channel near 11 μm to high temperature is relatively slow [25]. The use of satellites to monitor forest fires is distinguished by this change. Therefore, the 7-channel mid-infrared and 14-channel long-wave infrared in the Himawari-8 AHI sensor can be used for fire detection. The center wavelength of the 7-channel 3.9 μm is consistent with the center wavelength of the MODIS fire channel 21, which can be used to identify small fire spots and intensity levels. The 14-channel (11.2 μm) has a stable ground emissivity, which can better show the ground temperature of various coverage types. At the same time, the reflectance information of channels 1, 3, 4, and 5 and the brightness temperature information of channels 7, 14, and 16 are used to identify clouds, filter out flares, and eliminate false alarms. Among them, for channels with different resolutions, the resample tool in ArcGIS is used to unify the resolution.

The research data is full-scale observation data of Himawari-8 L1 NC (Network Common Data Format) and downloaded from the Japan Meteorological Agency. After downloading, it was preprocessed by channel extraction, brightness temperature calculation, cropping and other ways for forest fire discrimination. The data of land use type are from the 2020 report of land use data in China downloaded from the website of the Resource Environmental Science and Data Center of the Chinese Academy of Sciences (http://www.resdc.cn). The verification data select the data from the China Forest and Grassland Fire Fighting Network. The data include information such as the time, location, pixel size, report type, and monitoring satellite of the forest fire. The verification data also selects the fire point product data of Himawari-8 released by Japan Meteorological Agency, and the data can be downloaded from its ftp server. Product data are divided into rail products (Level-2), 1-hour products (Level-3), 1-day products (Level-3) and 1-month products (Level-3). This study uses 1-day products (Level-3) to compare and validate the algorithm adopted in the current study. This study also uses sentinel-2A data to observe and verify forest fires.

TABLE 1. Himawari-8 AHI spectrical features.

Channel No.	Wavelength (μm)	Spatial Resolution (km)	Observation object
1	0.46	1.0	Ocean, vegetation, atmospheric environment
2	0.51	1.0	Ocean, vegetation, atmospheric environment
3	0.64	0.5	Land, cloud
4	0.86	1.0	Ocean, vegetation
5	1.60	2.0	Land, cloud and snow
6	2.30	2.0	Cloud
7	3.90	2.0	Land and surface, surface temperature
8	6.20	2.0	Cirrus, water vapour
9	7.00	2.0	Ocean, vegetation
10	7.30	2.0	Ocean, vegetation
11	8.60	2.0	Ocean, vegetation
12	9.60	2.0	Water vapour
13	10.40	2.0	Land and surface, surface temperature
14	11.20	2.0	Land and surface, surface temperature
15	12.30	2.0	Land and surface, surface temperature
16	13.30	2.0	Surface temperature

III. PROPOSED ALGORITHM DESCRIPTION

At present, the contextual method is the most widely used method for identifying forest fire points. It mainly consists of two basic steps: the first step is to set a threshold to find out potential fire point pixels. Its threshold is relatively looser than the fixed threshold method since it aims to prevent

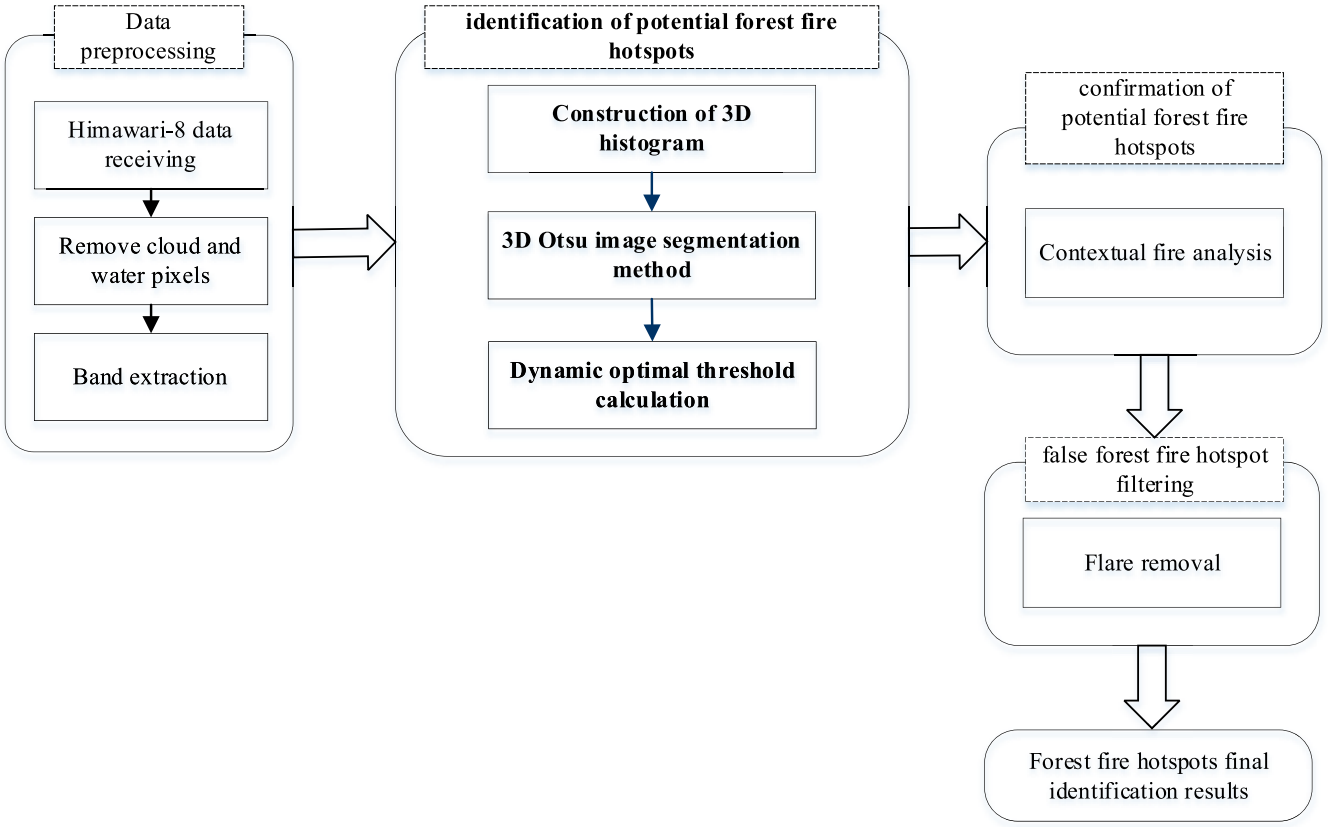

FIGURE 2. Flow chart of forest fires recognition algorithm based on Himawari-8.

missing fire points. The second step is to adjust the threshold to identify the confirmed fire point in the potential fire point pixel. In order to reduce the error caused by a fixed threshold in the first step, this paper starts with using the three-dimensional Otsu image segmentation method before using the contextual method. This method can automatically calculate the segmentation threshold of the potential forest fire points. The flow chart of the proposed approach is shown in Figure 1. The detailed calculation process can be divided into four main steps: data preprocessing, identification of potential forest fire points, confirmation of potential forest fire points, and false forest fire point filtering.

A. DATA PREPROCESSING

1) CLOUND PIXEL IDENTIFICATION

In this paper, a multi-spectral comprehensive threshold cloud detection algorithm is adopted [26]. This algorithm is based on Himawari-8 and uses different thresholds of reflectivity and brightness temperature in different channels to detect thick clouds, high clouds, and medium-low clouds. At the same time, the study adopts the clear sky restoration algorithm to check and correct the detection results:

Identify thick cloud conditions:

$$\rho_{03} > 0.3 \tag{2}$$

$$0.9 < \frac{\rho_{04}}{\rho_{03}} < 1.1 \tag{3}$$

Identify high cloud conditions:

$$BT_{16} < 236K \tag{4}$$

$$0.09 < \frac{\rho_{03} - \rho_{05}}{\rho_{03} + \rho_{05}} < 0.2 \quad and \ \rho_{01} > 0.1 \tag{5}$$

Identify medium and low cloud conditions:

$$BT_{14} < 278K \tag{6}$$

$$BT_7 - BT_{14} > 20K \tag{7}$$

Perform clear sky repair on the identified cloud pixels:

$$-0.18 \leq NDVI \leq 0.2 \tag{8}$$

where: ρ is the apparent reflectance of a certain channel of AHI, BT is the brightness temperature of a certain channel of AHI, $NDVI$ is the normalized difference vegetation index.

2) WATER PIXEL IDENTIFICATION

It is obvious that water cannot cause a fire because of its natural characteristics. The light spot on the water body is a flare that would appear when the water body forms a certain angle with the sun. In order to reduce the influence of flares on forest fire points identification, water pixels must be excluded. Therefore, this study uses the 2020 report of land use data in China to identify water pixels. The report is downloaded from the website of the Resource Environmental Science and Data Center of the Chinese Academy of Sciences

(http://www.resdc.cn). The land use of Yunnan Province has been shown in Figure 3. The original resolution of the product data is 30m. After resampling in ArcGIS, it can meet the requirements of this research. The forest fire points recognition algorithm proposed in this paper does not process any pixels that are recognized as clouds or water.

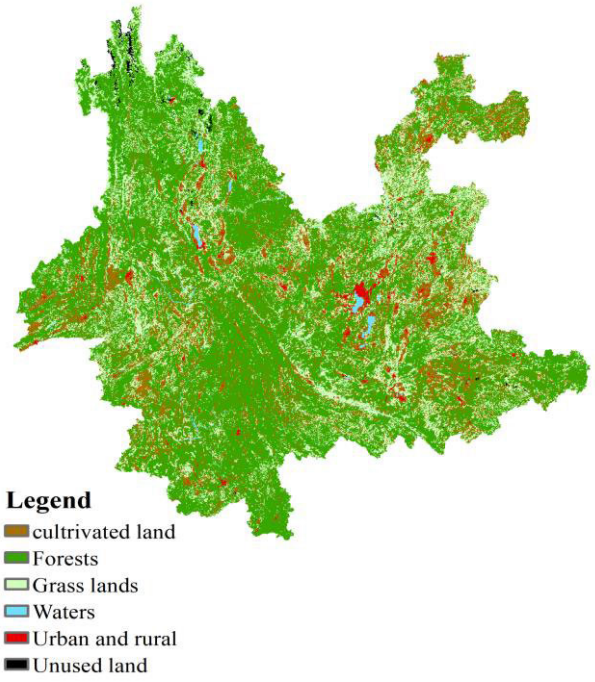

FIGURE 3. Distribution map of the underlying surface types in Yunnan province.

B. POTENTIAL FOREST FIRE IDENTIFICATION

A pixel is considered as potential forest fire pixel if it satisfies the following condition:

$$T_7 > T_7^* \tag{9}$$

$$\Delta T > \Delta T^* \tag{10}$$

where $\Delta T = T_7 - T_{14}$, and T_7^*, ΔT^* are thresholds for potential forest fire identification.

The potential forest fire points could be monitored through image segmentation as the segmentation threshold has fully applied different regions and different environmental conditions. In this paper, the basic idea of the 3d otsu algorithm is to construct a 3d histogram, use the 3d otsu method for segmentation, obtain an adaptive segmentation threshold, and separate potential forest fire hot pixels from the background pixels, as shown below.

1) CONSTRUCTION OF 3D HISTOGRAM DISTRIBUTION

Suppose the image size scanned by the remote sensing satellite himawari-8 is M×N. The coordinate of the forest fire point is (x,y), the gray value of the forest fire point is defined as $f(x,y)$, $g(x,y)$ is the neighborhood average gray level of $k \times k$, and $h(x,y)$ is the neighborhood variance gray level of $k \times k$, then

$$g(x,y) = \frac{1}{k*k} \sum_{m=-(k-1)/2}^{(k-1)/2} \sum_{n=-(k-1)/2}^{(k-1)/2} f(x+\mathrm{m}, y+n) \tag{11}$$

$$h(x,y) = (f(x,y) - g(x,y))^2 \tag{12}$$

The 3D histogram is limited in the cube region of a size of $L \times L \times L$. By using the 3D vector $[f(x,y),g(x,y),h(x,y)]$ to express a Himawari-8 image and letting r_{ijk} be the total occurrence frequency of pair (i,j,k), Where $i = f(x,y)$, $j = g(x,y)$, $k = h(x,y)$. Since the saturation temperature of channel 7 is 500K, and the brightness temperature of non-cloud pixels is greater than 270K, any point on the histogram is denoted as:

$$P_{ijk} = \frac{C_{ijk}}{M \times N} \tag{13}$$

where $i, j = 270, \ldots, 500$.

2) OPTIMAL THRESHOLD CALCULATION OF 3D OTSU

Now suppose that the pixels are partitioned into classes C_0 and C_1 (forest fire points and background) by a threshold pair(s, t, q). The probabilities of C_0 and C_1 are:

$$\omega_0 = \sum_{(i,j,k)\in C_0} P_{ijk} = \sum_{i=0}^{s}\sum_{j=0}^{t}\sum_{k=0}^{q} P_{ijk} \tag{14}$$

$$\omega_1 = \sum_{(i,j,k)\in C_1} P_{ijk} = \sum_{i=s+1}^{L-1}\sum_{j=t+1}^{L-1}\sum_{k=q+1}^{L-1} P_{ijk} \tag{15}$$

C_0 and C_1 correspond to the mean value:

$$\begin{aligned}\mu_0 &= (\mu_{0i}, \mu_{0j}, \mu_{0k})^T \\ &= \left(\frac{1}{\omega_0}\sum_{i=0}^{s}\sum_{j=0}^{t}\sum_{k=0}^{q} iP_{ijk}, \frac{1}{\omega_0}\sum_{i=0}^{s}\sum_{j=0}^{t}\sum_{k=0}^{q} jP_{ijk}, \right. \\ &\quad \left. \frac{1}{\omega_0}\sum_{i=0}^{s}\sum_{j=0}^{t}\sum_{k=0}^{q} kP_{ijk}\right)^T\end{aligned} \tag{16}$$

$$\begin{aligned}\mu_1 &= (\mu_{1i}, \mu_{1j}, \mu_{1k})^T \\ &= \left(\frac{1}{\omega_1}\sum_{i=s+1}^{L-1}\sum_{j=t+1}^{L-1}\sum_{k=q+1}^{L-1} iP_{ijk}, \frac{1}{\omega_1}\sum_{i=s+1}^{L-1}\sum_{j=t+1}^{L-1}\sum_{k=q+1}^{L-1} jP_{ijk}, \right. \\ &\quad \left. \frac{1}{\omega_1}\sum_{i=s+1}^{L-1}\sum_{j=t+1}^{L-1}\sum_{k=q+1}^{L-1} kP_{ijk}\right)^T\end{aligned} \tag{17}$$

The total mean vector of the 3D histogram is:

$$\begin{aligned}\mu_T &= (\mu_{Ti}, \mu_{Tj}, \mu_{Tk})^T \\ &= \left(\sum_{i=0}^{L-1}\sum_{j=0}^{L-1}\sum_{k=0}^{L-1} iP_{ijk}, \sum_{i=0}^{L-1}\sum_{j=0}^{L-1}\sum_{k=0}^{L-1} jP_{ijk}, \sum_{i=0}^{L-1}\sum_{j=0}^{L-1}\sum_{k=0}^{L-1} kP_{ijk}\right)^T\end{aligned} \tag{18}$$

The discrete measure matrix between the target class and background class could be expressed as:

$$S_B = \omega_0\left[(\mu_0-\mu_T)(\mu_0-\mu_T)^T\right]+\omega_1\left[(\mu_1-\mu_T)(\mu_0-\mu_T)^T\right] \tag{19}$$

The 3D Otsu method uses the trajectory of S_B as their dispersion criterion,

$$\begin{aligned} t_r S_B &= \omega_0\left[(\mu_{0i}-\mu_{Ti})^2+\left(\mu_{0j}-\mu_{Tj}\right)^2+(\mu_{0k}-\mu_{Tk})^2\right] \\ &\quad +\omega_1\left[(\mu_{1i}-\mu_{\pi})^2+\left(\mu_{1j}-\mu_{Tj}\right)^2+(\mu_{1k}-\mu_{Tk})^2\right] \\ &= \frac{[\mu_i-\omega_0\mu_{Ti}]^2+\left[\mu_j-\omega_0\mu_{Tj}\right]^2+[\mu_k-\omega_0\mu_{Tk}]^2}{\omega_0\left(1-\omega_0\right)} \end{aligned} \tag{20}$$

Choose a threshold vector (S, T, Q) by maximizing:

$$t_r S_B(S,T,Q) = \max_{270<s,t,q<500}\{t_r S_B(s,t,q)\} \tag{21}$$

In the previous forest fire point recognition algorithm, T_7^* was usually set as fixed value at 315K or 320K (305K at night), and ΔT^* was usually set as fixed value of 20K (10K at night). In order to reduce the omission error, the dynamic threshold T_7^* should be lower than the fixed threshold. In the 3D histogram distribution above, S represents the surface temperature value of a pixel, T represents the average surface temperature in adjacent area, and Q represents the adjacent variance of the ground surface temperature. The temperature value, adjacent average value, and adjacent variance of any pixel in the image will be very similar; by contrast, those of the pixels between the edges of forest fire points and that of non-forest fire points are different. Therefore, the potential forest fire points threshold is calculated separately based on each sample location.

$$T^* = \min\{S, 315K\} \tag{22}$$

$$\Delta T^* = \max\{S-T, \overline{\Delta T}\} \tag{23}$$

where $\overline{\Delta T}$ is the mean value of ΔT among the neighborhood pixels.

C. CONFIRMATION OF FOREST FIRE POINTS

MODIS data has a dedicated fire detection channel, and its fire detection algorithm is developed on the basis of the AVHRR fire point algorithm. So far, the MODIS fire point identification algorithm has been developed to the sixth version, and the daily global misclassification error of its product data is 1.2%, which is lower than the 2.4% of the fifth version [27]. Based on this, the method of confirming the fire point pixel of the algorithm in this paper is as follows:

Daytime: Those who meet the conditions {A or [B and C and D and (E or F)]} are recognized to be a fire, otherwise it is a non-fire.

Night: Those who meet the condition [A or (B and C and D)] are recognized to be a fire point, otherwise it is a non-fire spot.

$$\text{A}: T_7 > 360K(\text{Night } 320K) \tag{24}$$

$$\text{B}: \Delta T > \overline{\Delta T} + 3.5\delta_{\Delta T} \tag{25}$$

$$\text{C}: \Delta T > \overline{\Delta T} + 6K \tag{26}$$

$$\text{D}: T_7 - \overline{T_7} > 2\delta_7 \tag{27}$$

$$\text{E}: T_{14} - \overline{T_{14}} > 2.5\delta_{14} \tag{28}$$

$$\text{F}: \delta_7' > 5K \tag{29}$$

In the formula, T_7 and T_{14} are Himawari data 3.9μm and 11.2μm channel temperature. T_7 and T_{14} are the average temperature of 3.9μm and 11.2μm in the background window. $\Delta T = T_7 - T_{14}$, which is the temperature difference between 3.9μm and 11.2μm. $\overline{\Delta T}$ is the average temperature difference between 3.9μm and 11.2μm in the background window. δ_7 and δ_{14} are the temperature standard deviations of 3.9μm and 11.2μm in the background window. $\delta_{\Delta T}$ is the standard deviation of the temperature difference between 3.9μm and 11.2μm in the background window. δ_7' is the 3.9μm standard deviation of the fire point pixel in the background window.

D. FALSE FOREST FIRE POINT FILTERING

When the fire pixel is identified, it is necessary to perform flare identification to reduce this type of errors. The identification principle is as followed: if the visible light and infrared reflectivity are both greater than 0.3, and the flare angle θ_r is less than 30°, then the pixel is identified as a flare. The flare angle [28] is calculated as:

$$\cos\theta_r = (\cos(\theta_V)\cos(\theta_s) - \sin(\theta_v)\sin(\theta_s)\cos(\psi)) \tag{30}$$

where: θ_v and θ_s are the observation zenith angle and solar zenith angle, respectively. ψ is the relative azimuth. θ_r is the angle between the vector pointing from the ground to the satellite and the direction of the specular reflection.

IV. RESULTS AND DISCUSSION

When forest fire points are identified in a traditional way, which might be influenced by regions and seasons, there are possible omissions or wrong classifications. In order to reduce the omission caused by fixed forest fire points pixel recognition threshold, this article first set up windows to monitor potential forest fire points according to different regions and different environmental conditions. In order to ensure that the background information is fully utilized, the window size set 21 × 21 pixels [21]. As shown in Figure 4, the selected study area is Yunnan Province, which contains 251 sub-regions, each of which contains 21 × 21 pixels. After performing a 3D Otsu image segmentation on each sub-region, it is possible to obtain the potential forest fire point monitoring threshold for each sub-region. The correlation coefficient R^2 between the segmentation threshold of potential forest fire points and latitude obtained in this paper is 0.77. Observing Figure 5, we can see that as the latitude increases, the threshold of potential forest fire points gradually decreases. This is because the closer to the equator, the higher the surface temperature. The algorithm makes full use of the information of neighboring pixels and can be flexibly applied to regions of different latitudes.

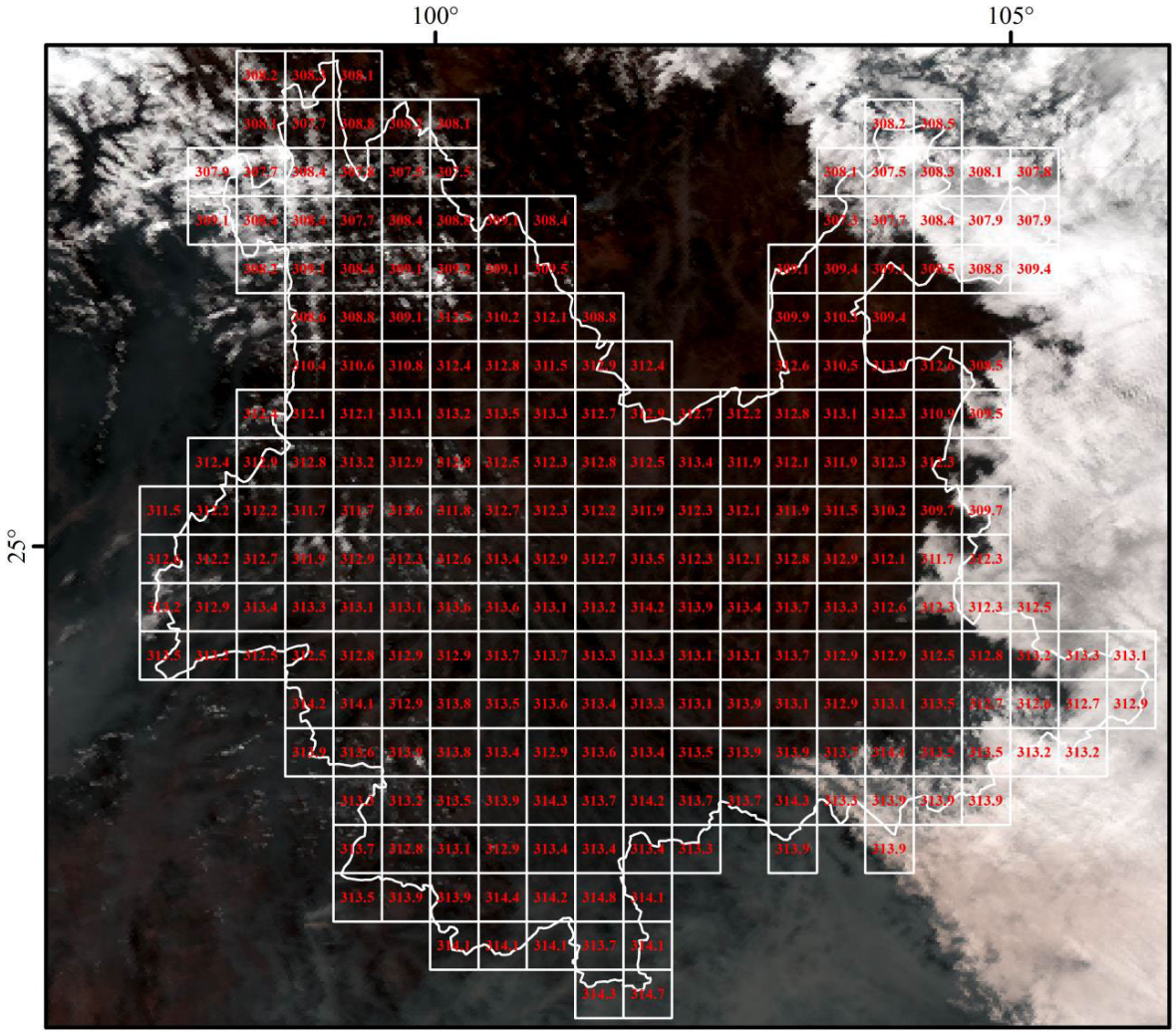

FIGURE 4. Identification threshold of potential forest fires in Yunnan Province. The red numbers represent the potential fire threshold segmented by the 3D Otsu method.

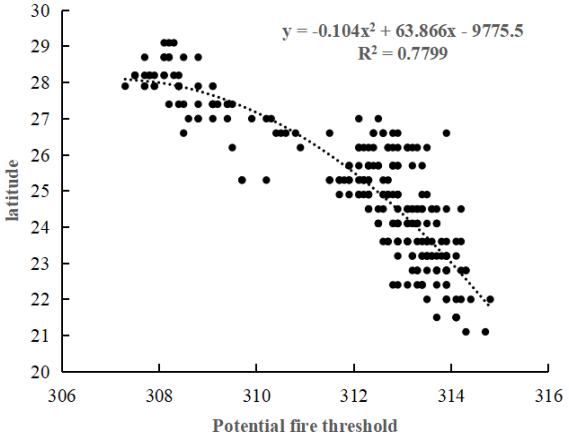

FIGURE 5. Correlation graph between potential forest fire threshold and latitude.

The results of potential fire spot recognition overlaps on the image of the study area. Figure 6(a) shows the potential forest fire points pixels identified by the traditional contextual monitoring algorithm. Figure 6(b) presents the potential forest fire point pixels identified according to the algorithm in this paper. Using the JAXAWLF (Wild Land Fire) 1-day product data (Level-3) introduced by the Japan Meteorological Agency to compare with the results of this article, it is possible to see difference between the two algorithms at the circle in the figure. At the green circle, the traditional contextual identification algorithm does not detect the low temperature braising point, which is included in the detection using 3D Otsu algorithm. By using 3D Otsu algorithm, the potential forest fire points thresholds in the green circle are T_7^* (312.1 K) and ΔT^* (12.0K). At the blue circle, the traditional contextual identification algorithm is missing the high temperature fire point, which is included in the detection using 3D Otsu algorithm. The potential forest fire points thresholds in the blue circle are T_7^* (315 K) and ΔT^* (22.3K). Therefore, the 3D Otsu algorithm can provide more comprehensive results, including low-temperature simmering points and high-temperature fire point combustion.

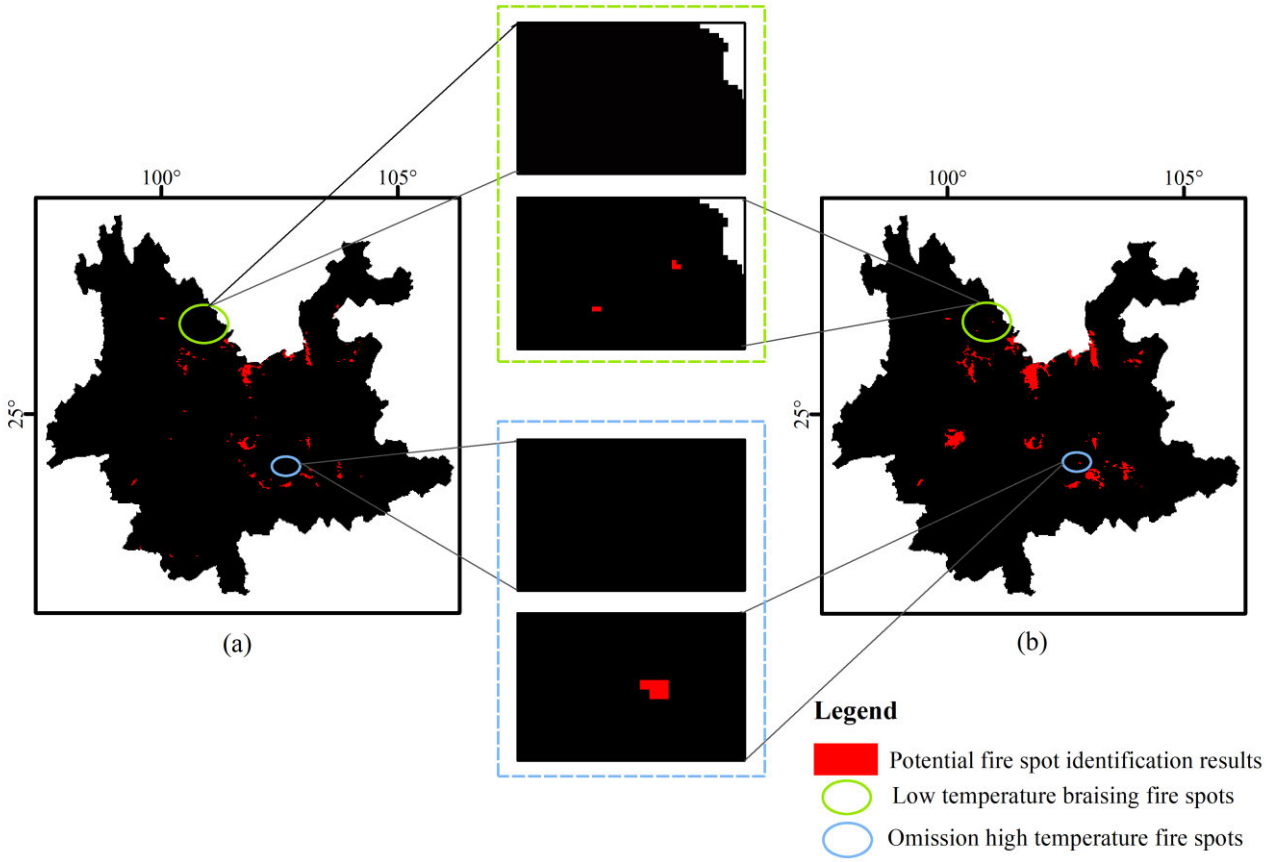

FIGURE 6. Comparison chart of identification results of potential forest fire points at 5:00 on March 30, 2020 (13:00 Beijing time).

In order to better display the characteristic of forest fire points and enhance the original satellite monitoring images, this article selects the following channels to obtain the false color image: Channel 7 is used as the red channel, Channel 14 is used as the green channel, and Channel 15 is used as the blue channel. Then we adopt context method to confirm the existence of potential forest fire points in sub-regions, and overlay the confirmed forest fire points on the false color image of Yunnan Province, as shown in Figure 7(a).

In order to analyze the forest fire point monitoring results more clearly, this study extracts the mid-infrared channel image with the identified fire spot in Yunnan Province as a mask. The result is shown in Figure 7(b). According to the fire product data provided by Himawari-8, it can be seen that forest fires occurred in place 1 and place 2. In order to verify forest fires more clearly, we use high-resolution images (Sentinel-2A data) to observe forest fires. Figure 7(c) and Figure 7(d) show the forest fires in place 1 and place 2 respectively. Figure 7(e) is a false color image of the fire in Yunnan Province. Figure 7(f) reveals the limitation of traditional context method, as it only identifies one high temperature fire spot, with omitting low temperature fire spot in place 2.

By contrast, Figure 7(g) is the result after using current algorithm, and it successfully presents the high temperature fire point in place 1.At the same time, by using 3D Otsu algorithm, the study identified the potential forest fire points thresholds in place 2, which are T_7^* (312.1 K) and ΔT^* (12.0K). Followed by using contextual method to confirm the fire point, the study can located and monitor the low-temperature braising fire points in place 2. It can be seen that, different from traditional methods, the algorithm in this paper can accurately locate and monitor the real high temperature fire point, as well as low temperature braising fire point near the high temperature point.

In order to quantify the accuracy of the algorithm in this paper, the accuracy rate (P), the omission errors rate (M), and the comprehensive value (F) of the accuracy rate and the omission errors rate are used to carry out the evaluation in a unified way [29]. The specific formula is as follows:

$$P = \frac{Y_y}{Y_y + Y_n} \tag{31}$$

$$M = \frac{N_y}{Y_y + N_y} \tag{32}$$

$$F = \frac{2P(1-M)}{1+P-M} \tag{33}$$

where: Y_y is the number of real fire points detected, Y_n is the number of falsely detected fire points, N_y is the number of missed fire points, P and M are the accuracy rate

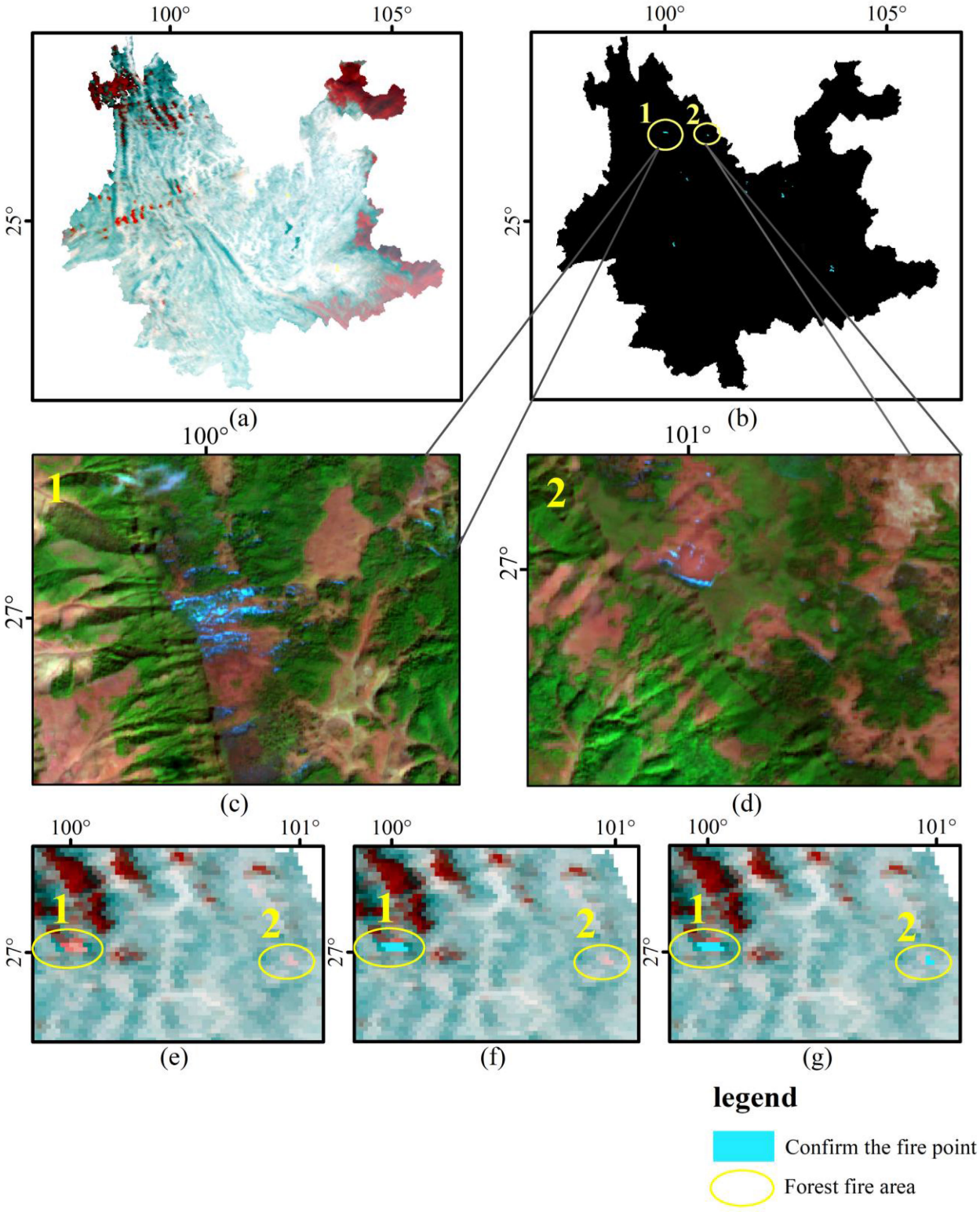

FIGURE 7. Analysis of the forest fires points after confirmation. (a) The false color map of the confirmed fire spot in Yunnan Province. (b) The result of the mid-infrared channel image extracted with the recognition result of the confirmed fire point in Yunnan Province as a mask. (c) High temperature forest fires of place 1 observed by Sentinel-2A. (d) Low-temperature braising forest fires of place 2 observed by Sentinel-2A. (e) False color images of two confirmed fire spot examples. (f) Two examples of confirmed fire points identified by the algorithm prior to the improvement. (g) Two examples of confirmed fire points identified by the improved algorithm.

and the omission errors respectively, F a is the comprehensive evaluation index of accuracy rate and missed detection rate.

According to the report from China Forest and Grassland Fire Fighting website, there were 22 forest fires occurred in Yunnan Province from 16:00 on March 30, 2020 to 16:00 on

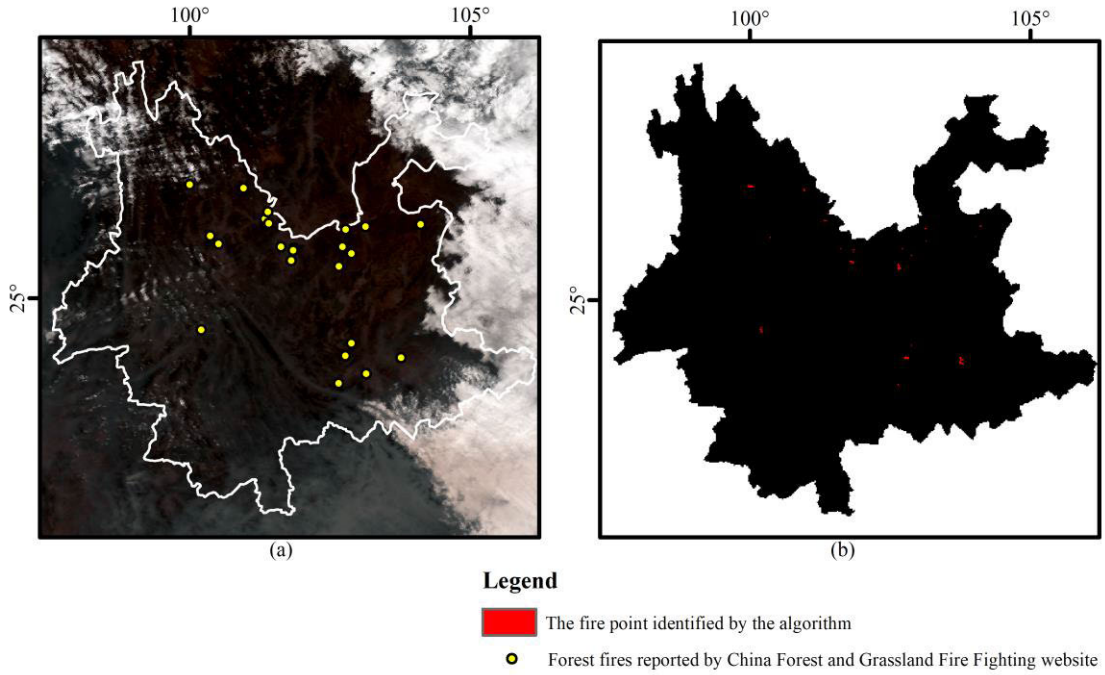

FIGURE 8. Comparison chart between the forest fire of validation datasets and the fire point by the algorithm. (a)The forest fires reported by China Forest and Grassland Fire Fighting website. (b) The forest fires identified by the improved algorithm.

TABLE 2. Accuracy evaluation of discrimination results.

Forest fire point data	Correct rate	Omission errors rate	F
China Forest and Grassland Fire Fighting website data	0.79	0.14	0.82
WLF-daily product data	0.84	0.24	0.8

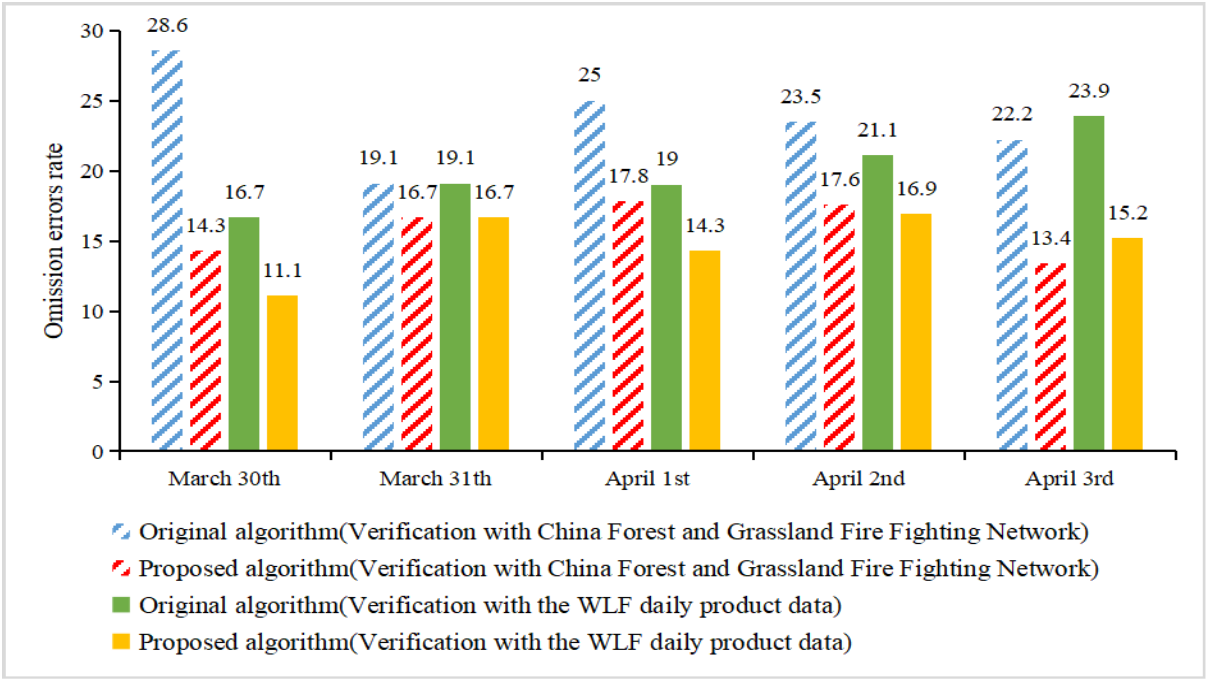

FIGURE 9. The omission errors rate of forest fire points in this paper's algorithm from March 30 to April 3, 2020 in Yunnan Province.

April 1, 2020. Through comparative analysis of Figure 8, 19 of the 24 forest fires identified by the algorithm in this paper are consistent with the report from China Forest and Grassland Fire Fighting website. The possible reason for the three unidentified fires might be the undetected size of fire or unduly cloud covering, etc. It can be seen from Table 2 that

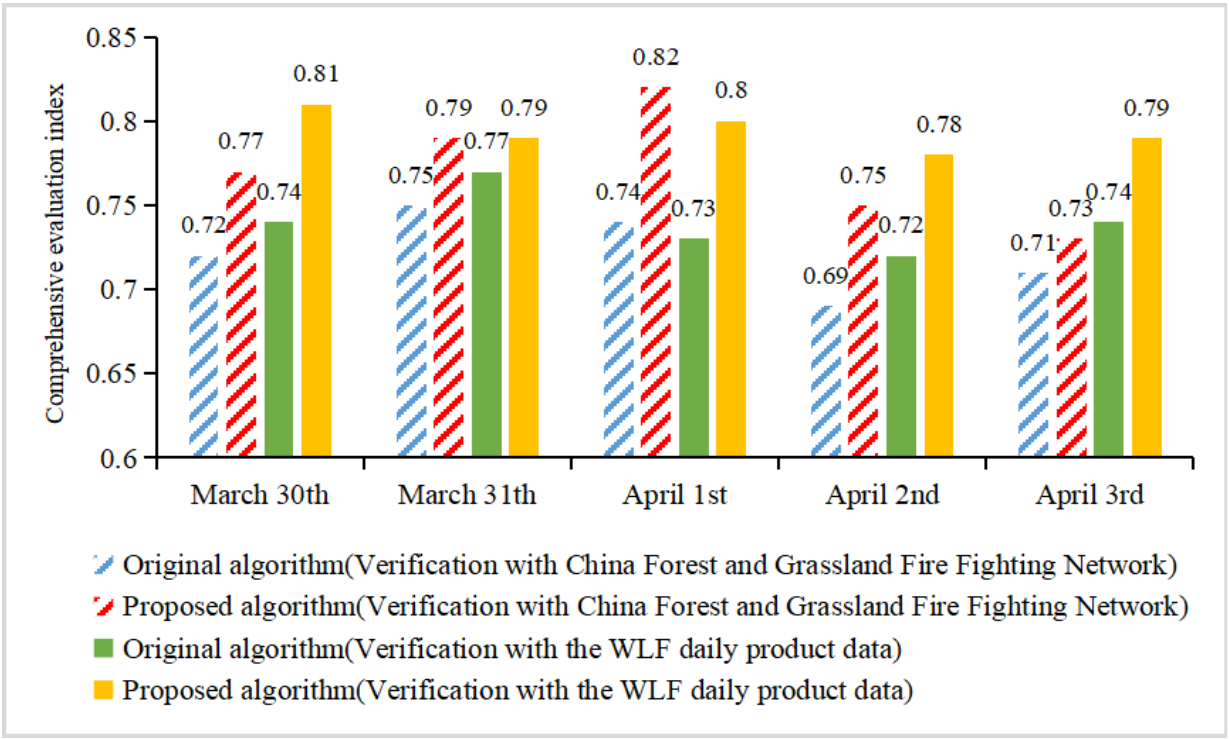

FIGURE 10. Comprehensive evaluation index of forest fire points in this paper's algorithm from March 30 to April 3, 2020 in Yunnan Province.

the identification rate of algorithm adopted by this study is as accurate as that of data from China Forest and Grassland Fire Fighting website, reaching 0.79, with the omission rate 0.14 and the comprehensive evaluation value 0.82. It shows that the results from the current study are highly consistent with that from the Chinese Forest and Grassland Firefighting website.

Similarly, the consistency can be seen from comparing the JAXAWLF (Wild Land Fire) 1-day product data (Level-3) launched by the Japan Meteorological Agency and the results processed by algorithm of this paper. In the 1-day product data (Level-3) on April 1, 2020, a total of 181 fire spots can be found in Yunnan Province. In the result of the proposed algorithm, 137 out of 163 fire spots are in line with the WLF daily product data. For the inconsistency of the methods, the possible explanation could be that false fire points have been detected, etc. It can be seen from Table 2 that the accuracy of the result is 0.84, which is the same as the WLF daily product data. The missed detection rate for both is 0.24, and the comprehensive evaluation value of the accuracy and missed detection rate is 0.8, indicating that the two have high consistency and can be used to identify fire spots.

In order to test the accuracy of the algorithm in different periods, this paper uses data from March 2020 to April 2020 in current research. Figure 9 shows the detailed comparison of the omission rate of between the old and current algorithms. It can be seen that on March 30 and April 3, when the number of fires was small, the omission rate of the current algorithm dropped by about 10%. During the period from March 31 to April 2, the omission rate of the algorithm dropped by about 5% compared with the previous change. This is due to the large number of fires during this period. Therefore, the algorithm in this paper is more sensitive to small-scale forest fire events, which can greatly reduce the omission of forest fire point monitoring. Figure 10 shows the detailed comparison of the comprehensive evaluation value, showing that the comprehensive evaluation value of the algorithm in this paper is about 5% higher than before. However, the comprehensive evaluation value verified with WLF daily product data is generally greater than the comprehensive evaluation value verified with the data from the China Forest and Grassland Fire Fighting website. This might be caused by different types of data, since on the China Forest and Grassland Fire Fighting website, only original remote sensing image data can be found, instead of Himawari-8 data. Another reason could be the difference in imaging time. In general, the algorithm in this paper has higher accuracy, and can be applied to other remote sensing image data at the same time.

V. CONCLUSION

This research is based on the Himawari-8 geostationary satellite data, using the 3D Otsu image segmentation method, combined with the contextual method to confirm the fire point, and thus it improves the traditional forest fire identification algorithm. The following conclusions can be drawn: (1) The 3D Otsu image segmentation method can be used to automatically select the threshold of potential fire points, which fully considers the information of neighboring pixels,

and avoids poor applicability of the fixed threshold method in different regions. (2) The algorithm in this paper can accurately monitor low-temperature forest fire points. Because it is very sensitive to small-scale forest fires, it reduces the omissions of forest fire points monitoring, enabling timely identification of forest fires in the early stage, and gaining valuable time for firefighting and rescue.

REFERENCES

[1] P. J. Crutzen, L. E. Heidt, J. P. Krasnec, W. H. Pollock, and W. Seiler, "Biomass burning as a source of atmospheric gases CO, H_2, N_2O, NO, CH_3Cl and COS," *Nature*, vol. 282, no. 5736, pp. 253–256, Nov. 1979.
[2] W. Booth, "Monitoring the fate of the forests from space," *Science*, vol. 243, no. 4897, pp. 1428–1429, Mar. 1989.
[3] L. Giglio, J. Descloitres, C. O. Justice, and Y. J. Kaufman, "An enhanced contextual fire detection algorithm for MODIS," *Remote Sens. Environ.*, vol. 87, nos. 2–3, pp. 273–282, Oct. 2003.
[4] L. Giglio, W. Schroeder, and C. O. Justice, "The collection 6 MODIS active fire detection algorithm and fire products," *Remote Sens. Environ.*, vol. 178, pp. 31–41, Jun. 2016.
[5] W. Chen, Y. Zhou, J. Chen, E. Zhou, W. Zhou, and S. Sui, "Wildfire monitoring technology of transmission lines based on Himawari-8 geostationary meteorological satellite," in *Proc. IEEE 3rd Conf. Energy Internet Energy Syst. Integr. (EI)*, Nov. 2019, pp. 2408–2412, doi: 10.1109/EI247390.2019.9061748.
[6] NESDIS, NOAA. (Oct. 11, 2013). *GOES-R Advanced Baseline Imager (ABI) Algorithm Theoretical Basis Document for Fire/Hot Spot Characterization, Version 2.6*. [Online]. Available: https://www.meteorologia.gov.py/satelite-goes-16/ATBD_GOES-R_FIRE_v2.6_Oct2013.pdf
[7] G. J. Roberts and M. J. Wooster, "Fire detection and fire characterization over Africa using Meteosat SEVIRI," *IEEE Trans. Geosci. Remote Sens.*, vol. 46, no. 4, pp. 1200–1218, Apr. 2008.
[8] Z. Xie, "Research on fire detection and exploration of automated cloud detection based on Himawari-8 remote sensing," Ph.D. dissertation, Dept. Safety. Sci. Eng., Univ. Sci. Technol. China, Anhui, China, 2019.
[9] X. Huang, "Research on fire point monitoring with high time and high spatial resolution based on multi-source remote sensing data," M.S. thesis, Dept. Inst. Eng., Univ. Automation Eng., Sichuan, China, 2020.
[10] Y. X. Xing, D. F. Nan, and L. Yu, "Research and development of forest fire risk early warning system," *Comput. Knowl. Technol.*, vol. 7, no. 3, pp. 3923–3927, 2011.
[11] J. Pan, L.-X. Xing, J.-C. Wen, T. Meng, and L.-J. Jiang, "Inversion method study on short wave infrared remote sensing data high temperature surface feature temperature," in *Proc. 2nd Int. Congr. Image Signal Process.*, Oct. 2009, pp. 1–4.
[12] C. Filizzola, R. Corrado, F. Marchese, G. Mazzeo, R. Paciello, N. Pergola, and V. Tramutoli, "RST-FIRES, an exportable algorithm for early-fire detection and monitoring: Description, implementation, and field validation in the case of the MSG-SEVIRI sensor," *Remote Sens. Environ.*, vol. 192, pp. e2–e25, Apr. 2017.
[13] Z. Jie, "An improved algorithm for forest fire detection: A study on brightness temperature, vegetation index and AOD," *Remote Sens. Technol. Appl.*, vol. 31, no. 5, pp. 886–892, 2016.
[14] M. D. Flannigan and T. H. V. Haar, "Forest fire monitoring using NOAA satellite AVHRR," *Can. J. Forest Res.*, vol. 16, no. 5, pp. 975–982, 1986.
[15] S. P. Flasse and P. Ceccato, "A contextual algorithm for AVHRR fire detection," *Int. J. Remote Sens.*, vol. 17, pp. 419–424, Apr. 1996.
[16] Y. J. Kaufman, C. O. Justice, L. P. Flynn, J. D. Kendall, E. M. Prins, L. Giglio, D. E. Ward, W. P. Menzel, and A. W. Setzer, "Potential global fire monitoring from EOS-MODIS," *J. Geophys. Res.*, vol. 103, pp. 32215–32238, Dec. 1998.
[17] I. Csiszar, A. Abdelgadir, Z. Li, J. Jin, R. Fraser, and W. M. Hao, "Interannual changes of active fire detectability in North America from long-term records of the advanced very high resolution radiometer," *J. Geophys. Res.*, vol. 108, no. D2, pp. 4075–4085, 2003.
[18] R. Lasaponara, V. Cuomo, M. F. Macchiato, and T. Simoniello, "A self-adaptive algorithm based on AVHRR multitemporal data analysis for small active fire detection," *Int. J. Remote Sens.*, vol. 24, no. 8, pp. 1723–1749, Jan. 2003.
[19] X. Du, D. Cao, D. Mishra, S. Bernardes, T. Jordan, and M. Madden, "Self-adaptive gradient-based thresholding method for coal fire detection using ASTER thermal infrared data, Part I: Methodology and decadal change detection," *Remote Sens.*, vol. 7, no. 6, pp. 6576–6610, May 2015.
[20] T. Huang, G. Yang, and G. Tang, "A fast two-dimensional median filtering algorithm," *IEEE Trans. Acoust., Speech, Signal Process.*, vol. ASSP-27, no. 1, pp. 13–18, Feb. 1979, doi: 10.1109/TASSP.1979.1163188.
[21] X. Xiao, W. G. Song, Y. Wang, R. Tu, S. X. Liu, and Y. M. Zhang, "An improved method for forest fire spot detection based on variance between-class," *Spectrosc. Spectral Anal.*, vol. 30, no. 8, pp. 2065–2068, Aug. 2010.
[22] Z. Lin, Z. Wang, and Y. Zhang, "Optimal evolution algorithm for image thresholding," *J. Comput.-Aided Des. Comput. Graph.*, vol. 22, no. 7, pp. 1201–1206, Jul. 2010.
[23] G. Zhang, B. Li, J. Luo, and L. He, "A self-adaptive wildfire detection algorithm with two-dimensional Otsu optimization," *Math. Problems Eng.*, vol. 2020, pp. 1–12, Aug. 2020, doi: 10.1155/2020/3735262.
[24] P. Zhang, "The Chinese next-generation geostationary meteorological satellite FY-4 compared with the Japanese Himawari-8/9 satellites," *Adv. Meteorol. Sci. Technol.*, vol. 6, no. 1, pp. 72–75, Feb. 2016.
[25] L. Xiao, "A study on the application of EOS/MODIS in forest fire monitoring for Sichuan and Chongqing region," M.S. thesis, Dept. Geo-Eng., Southwest Jiaotong Univ., Sichuan, China, 2008.
[26] D. Pin, M. Liu, T. Xu, and Y. Song, "Application of Himawari-8 data in monitoring forest fire," *Acta Scientiarum Naturalium Universitatis Pekinensis*, vol. 6, no. 54, pp. 1251–1258, 2018.
[27] L. Giglio, W. Schroeder, and C. O. Justice, "The collection 6 MODIS active fire detection algorithm and fire products," *Remote Sens. Environ.*, vol. 178, pp. 31–41, Jun. 2016.
[28] S. Ri, "Real-time monitoring and early warning of grassland fire based on geostationary meteorological satellite," M.S. thesis, Dept. Geograph., Inner Mongolia Teaching Univ., Inner Mongolia, China, 2020.
[29] W. Yue, "Forest fire monitoring method and application based on remote sensing data," M.S. thesis, Dept Geograph., Nanjing Univ. Inf. Technol., Jiangsu, China, 2019.

ZHAO DENG received the B.S. degree in geographic information system from Hunan City University, Hunan, China, in 2019. She is currently pursuing the B.A. degree in forest management with Central South University of Forestry and Technology, Changsha, China. Her research interests include forest fire monitoring and disaster warning.

GUI ZHANG received the M.S. and Ph.D. degrees in forestry from Central South University of Forestry and Technology, Changsha, China. He is currently a second-level professor and a doctoral supervisor. He is also a Distinguished Professor of Asia–Europe Water Resources Research and Utilization Center and a Natural Disaster Emergency Management Expert of the People's Government of Hunan Province. He has authored or coauthored dozens of scientific articles and books. His research interests include forestry information engineering, ecological engineering, and disaster prevention and mitigation satellite application projects.